Frontiers in Heat and Mass Transfer (FHMT), 13, 5 (2019)
DOI: 10.5098/hmt.13.5

Global Digital Central
ISSN: 2151-8629

Frontiers in Heat and Mass Transfer

Available at www.ThermalFluidsCentral.org

INVESTIGATIONS OF WIRE-BONDED MICRO HEAT PIPES - A REVIEW

C. B. Sobhan[a] and G. P. Peterson[b*]

[a] *National Institute of Technology, Calicut, India 673601*
[b] *Georgia Institute of Technology, Atlanta, Georgia, USA 30332*

ABSTRACT

Micro heat pipes have found applications in numerous types of systems where effective heat dissipation in a limited space is required. One relatively new design/fabrication methodology for parallel micro heat pipes with high performance is referred to as "wire-bonded" micro heat pipe arrays. The following review analyzes the principles of operation of these devices and investigates the recent developments in the technology, along with their fabrication and application. The results indicate that these micro heat pipe arrays present an attractive alternative for a number of interesting applications, including many that have yet to be explored.

Keywords: *Micro Heat Pipes, Wire-bonded micro heat pipes, Micro Heat Pipe Modeling, Micro Heat Pipe Design*

1. INTRODUCTION

Micro heat pipes represent a potential design alternative for the development of compact, passive, high capacity heat removal systems with a very high effective thermal conductance. The individual micro heat pipes that comprise these systems do not employ a traditional wicking structure for the circulation of the working fluid, but rather depend upon small liquid arteries for the liquid return. They are typically comprised of a polygonal cross-sectional channel, with sharp corner regions, which when charged with a predetermined quantity of working fluid can result the transfer of significant amounts of thermal energy. In these devices, heat added to the evaporator section of an individual micro heat pipe, results in the vaporization of the working fluid, with the vapor flowing through the central portion of the channel cross-section, i.e., the vapor region. The return flow of the liquid condensed in the cooler section of the device results from the capillary forces occurring in the sharp corner regions of the passage, thus avoiding the need for a wick structure for liquid recirculation. Unlike conventional heat pipes, because of the relatively small feature size, the vapor and liquid flow in micro heat pipes are characterized by the varying cross-sectional areas of the liquid and to a lesser degree, the vapor flow regions. The required condition for successful micro heat pipe operation is that the average radius of the liquid-vapor meniscus formed in the corners of the channel is comparable in magnitude with the reciprocal of the hydraulic radius, which is the characteristic dimension of the total flow channel.

The operation and modeling of micro heat pipes have been examined in the literature along with discussions of the vapor continuum limits, (Cao *et al.,* 1993). An analysis of the capillary limit, which reveals that the disjoining pressure may play a role in the overall heat transfer was presented and indicates that this may be an important factor in determining the overall heat transfer capacity of an individual micro heat pipe.

A thermal analysis of individual micro heat pipe operation was conducted by Khrustalev and Faghri (1994) in which, a detailed mathematical model for a single micro heat pipe was developed, taking into consideration the liquid flow in the triangular shaped corners with polygonal cross-section. In this study, the predicted results were compared with the available experimental data.

A literature review of miniature and micro heat pipes was also presented by Cao and Faghri (1994), in which the importance of the longitudinal groove design on the heat transport capacity of miniature heat pipes was established. The vapor continuum limitation, which may prevent the successful operation of micro heat pipes under low or reduced working temperatures, along with a determination of the operating limits of a conventional heat pipe, were presented. Faghri (2002) conducted a review of the advances and challenges in micro/miniature heat pipes, which examines the advances in the determination of the heat transfer limitations and a thermal analysis of a number of the designs typically used in these devices.

The advances and challenges associated with the manufacturing and charging of these micro heat pipes was discussed by Cao and Faghri (2017) and included a review of micro and miniature heat pipes, emphasizing the importance of the design of the longitudinal grooves in increasing the heat transport capacity of these devices. Various micro heat pipe designs may be subjected to vapor continuum limitations under low working temperatures. The analysis of the capillary limit revealed that the disjoining pressure plays an important role in the heat transfer capacity of micro heat pipes.

The first steady-state model specifically designed for use in the modeling of micro heat pipes was developed by Cotter (1984). Building upon this model, Peterson (1988) and Babin *et al.* (1990) developed steady-state models for a trapezoidal micro heat pipe. The resulting model demonstrated that the capillary pumping pressure governed the maximum heat transport capacity of these devices. A comparative analysis of these two early models was performed by Gerner *et al.* (1992) resulting in the recognition that the capillary limit may never actually be reached due to instabilities occurring at the liquid-vapor interface. Longtin *et al.* (1994) developed a one-dimensional, steady-state model for the evaporator section of the micro heat pipe.

*Corresponding author. Email: bud.peterson@gatech.edu

An analytical model for etched, triangular micro heat pipes was first developed by Duncan and Peterson (1995), in which the curvature of the liquid-vapor meniscus in the evaporator could be calculated. In subsequent work, the hydraulic diameter was defined and incorporated the frictional effects of the liquid and the vapor. This model was expanded by Peterson and Ma (1996) to predict the minimum meniscus radius and maximum heat transport in triangular grooves. A detailed steady-state mathematical model for predicting the heat transport capability of a micro heat pipe, and the temperature gradients that contribute to the overall axial temperature drop as a function of the heat transfer was developed by Peterson and Ma (1999). A transient investigation of micro heat pipes was conducted by Wu and Peterson (1991) and Badran *et al.* (1993) developed a conjugate model to account for the transport of heat within the heat pipe and conduction within the heat pipe case.

A comprehensive review of the various types of heat pipes and their fabrication and operational characteristics, has been published by Faghri (2014), in which the construction and operation of individual micro heat pipes were examined in detail.

2. WIRE-BONDED MICRO HEAT PIPES

Wire-bonded micro heat pipes are flexible structures, fabricated by sandwiching an array of parallel wires between two flat metal sheets. A typical arrangement consists of an array of metallic wires sandwiched between two thin metal sheets forming flow passages in between. The bonding process consists of careful cleaning of the inner surface of the metal sheets to remove any oxidation and then heating the entire surface, while applying a uniform pressure to the surfaces of the two plates. In this way, the metal at the contact lines formed by the wires and the plates forms a bond creating the micro heat pipe structure with the liquid arteries occurring in the sharp corner regions at the junction of the wires and the plates.

Much like traditional micro heat pipes, these devices are evacuated and then charged with a predetermined amount of working fluid. The liquid flow within the sharp corner regions formed at the intersection of the wires and the plates is the result of the difference in the capillary radius in the evaporator and condenser regions. The vapor moves in the opposite direction through the interior portion of the channel. In the process of forming the vapor, the liquid absorbs heat through the heat pipe wall, which is then rejected in the cooler regions with the condensed vapor returning in the liquid flow passages.

The construction, operation and analysis of wire-bonded micro heat pipe devices has been described previously in the literature (Wang and Peterson, 2002a; Wang and Peterson, 2002b; Wang *et al.*, 2001; Peterson and Wang, 2003; Rag and Sobhan, 2009; Rag and Sobhan, 2010; Rag *et al.*, 2018). Although micro heat pipes do not, in general contain a formal wicking structure, as is the case for more conventional heat pipes, the fundamental operating principles and performance characteristics are similar and subject to the same limitations.

A typical micro heat pipe consists of the three fundamental sections, namely the evaporator, adiabatic section and the condenser. The high temperature and pressure developed at the evaporator section of the device forces the vapor to move to the cooler, condenser region. The sharp corners of the non-circular cross-sectional channels causes the flow of the liquid from the condenser to the evaporator, thus completing the flow cycle.

2.1 Preliminary Designs

The non-conventional design of micro heat pipes, referred to as 'wire-bonded' micro heat pipes was first presented and evaluated by Wang and Peterson (2002a), with a focus on advanced spacecraft applications. A bendable wire-bonded micro heat pipe array was fabricated by sintering a series of parallel aluminum wires between two parallel flat aluminum plates. This structure formed a contact line between the plates and the wires. The effects of the wire diameter, wire-pitch, number of wires and lengths of the adiabatic and condenser sections on the maximum heat transport capacity were evaluated and determined. A one-dimensional steady-state, analytical model for wire bonded micro heat pipe arrays was presented. This model considered the liquid-vapor interactions and the cross-sectional area variations to predict the optimum design parameters based on the predicted heat transfer performance. The numerical results based on the proposed model were validated experimentally. The wire diameter was found to influence the maximum heat transport capacity in a positive manner, indicating that the overall value was proportional to the square of the wire diameter. The maximum heat transport capacity was found to increase with the wire spacing, and indicated the existence of an optimal configuration.

Wang and Peterson (2002b) conducted optimization studies on wire-bonded micro heat pipe radiators using a combined numerical and experimental investigation, to optimize the heat transfer performance. It was noted that the wire spacing, radiator length and radiative characteristics of the surface, strongly influenced the maximum heat transport capacity of the radiator. An increase in the wire diameter was found to increase the temperature distribution, as well as the overall array efficiency. Experimental investigations with aluminum/acetone wire bonded micro heat pipe arrays indicated significant improvements in the temperature uniformity and overall radiation efficiency when compared to both solid conductors and uncharged versions.

The heat transfer performance and temperature distribution of the heat pipe array described above were predicted using a numerical model developed by Wang *et al.* (2001) by analyzing three configurations with and without a working fluid charge, using acetone as the working fluid, and comparing with actual working models. The radiator with the micro heat pipes was found to have an effective thermal conductivity 20 times that of the uncharged version, and 10 times a similarly sized solid material. The experimental tests conducted on these test articles illustrated that the effective conductivity was constant with respect to the temperature and that the heat transport capacity was proportional to the temperature difference between the evaporator and condenser. The flexible radiators, with the micro heat pipe arrays had an effective conductivity value of between 15 and 20 times that of the uncharged version, which resulted in a more uniform temperature distribution, thereby improving the overall radiation effectiveness.

Peterson and Wang (2003) analyzed a flat heat pipe thermal module consisting of a wire-bonded micro heat pipe for mobile computers. The performance analysis was accomplished using a thermal resistance model. Larger wire diameters were found to provide a significant increase in the maximum heat transport capacity.

Computational studies have been conducted on wire-bonded heat pipes to analyze their performance and to obtain the operational characteristics using numerical models (Rag and Sobhan, 2009; Rag and Sobhan, 2010; Rag *et al.*, 2018). The formulation and method of analysis used in these devices are presented here, with some typical results of the analysis.

2.2 Mathematical Model

The wire-bonded micro heat pipe array typically consists of a series of parallel heat pipe channels. Each of the individual heat pipe channels functions as an independent unit. The typical construction of the device is as shown in Fig. 1.

Each unit of the wire-bonded heat pipe array typically consists of an evaporator section where external heat is absorbed, and a cooled condenser section, with an adiabatic section in between, if necessary. In the analysis of this structure, a one-dimensional model is appropriate since the variations of the velocity, pressure and temperature would be

mostly one-dimensional in nature. The governing differential equations for the varying area domain of the channel of the wire bonded heat pipe have been formulated and solved, pertaining to both the vapor and liquid flow regions, to obtain the local and transient variations of the field variables, namely the velocity and the temperature of the working fluid.

The three distinct regions of a typical micro heat pipe are an externally heated evaporator, a condenser at the other end, which rejects heat by convection, and an adiabatic section that separates the two. Since the parameters vary prominently in the longitudinal direction, a one-dimensional mathematical model can be used in the analysis. The longitudinal variation in the cross-sectional areas of both the vapor and the liquid regions is incorporated in the analysis. The governing equations are formulated with the following assumptions:

1. Laminar flow in both the vapor and the liquid domains.
2. No-slip boundary conditions in both the liquid and the vapor flow domains.
3. Saturation conditions of the vapor.
4. Consistent meniscus radius of curvature at a given Longitudinal location.

The local meniscus radius, fluid pressure and surface tension are related by the Laplace-Young Equation. The mass, momentum and energy conservation equations at various sections, for both liquid and vapor, are utilized to obtain the velocity and temperature profiles.

In all of these equations, the area variations in the longitudinal direction can be expressed as a function of the local meniscus radius. The vapor pressure and temperature are related by the equation of state, and the vapor pressure values are reiterated in the vapor momentum equation for convergence. The Hagen-Poiseuille equation is used to calculate a first approximation of the liquid pressure, which is subsequently reiterated using the liquid momentum equation.

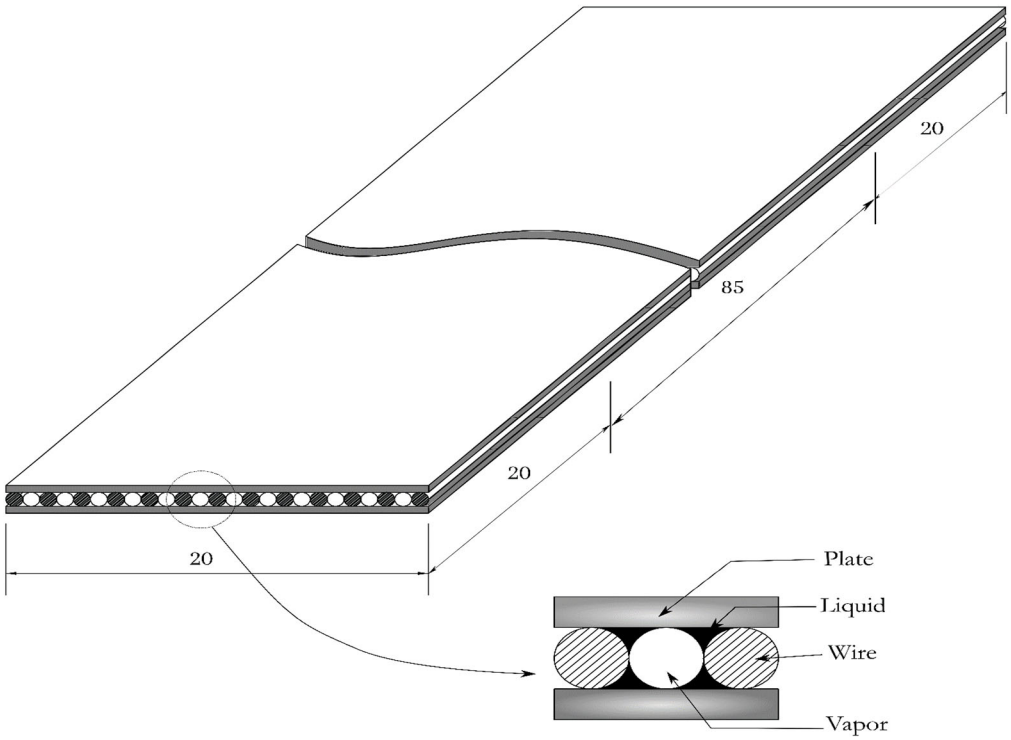

Fig. 1 Structure and cross-section of a typical wire-bonded micro heat pipe array

The mathematical formulation has been used to obtain the temperature and velocity distributions, as discussed in previous investigations (Rag and Sobhan, 2009; Rag and Sobhan, 2010; Rag *et al.*, 2018). The formulation steps of the problem are listed below for completeness.

The Laplace – Young Equation:

$$p_v(x) - p_l(x) = \frac{\sigma}{r(x)} \tag{1}$$

The vapor continuity equation:

For the evaporator section:

$$A_v \frac{du_v}{dx} + u_v \frac{dA_v}{dx} + P_{vi} v_{vi} = 0 \tag{2}$$

For the adiabatic section:

$$A_v \frac{du_v}{dx} + u_v \frac{dA_v}{dx} = 0 \tag{3}$$

For the condenser section:

$$A_v \frac{du_v}{dx} + u_v \frac{dA_v}{dx} - P_{vi} v_{vi} = 0 \quad (4)$$

The liquid continuity equation:

For the evaporator section:

$$A_l \frac{\partial u_l}{\partial x} + u_l \frac{\partial A_l}{\partial x} - P_{li} v_{li} = 0 \quad (5)$$

For the adiabatic section:

$$A_l \frac{\partial u_l}{\partial x} + u_l \frac{\partial A_l}{\partial x} = 0 \quad (6)$$

For the condenser section:

$$A_l \frac{\partial u_l}{\partial x} + u_l \frac{\partial A_l}{\partial x} + P_{li} v_{li} = 0 \quad (7)$$

The vapor momentum equation:

$$\rho_v \left[u_{v^2} \frac{\partial A_v}{\partial x} + 2 \frac{\partial u_v}{\partial x} A_v u_v \right] + A_v \frac{\partial p_v}{\partial x} + \rho_v A_v g \sin\theta - \frac{1}{2} \rho_v u_{v^2} P_{v_w} f_{vw} - \frac{1}{2} \rho_v u_{v^2} P_{v_i} f_{vi} = \rho_v A_v \frac{\partial u_v}{\partial t} \quad (8)$$

The liquid momentum equation:

$$-\rho_l \left[{u_l}^2 \frac{\partial A_l}{\partial x} + 2 A_l u_l \frac{\partial u_l}{\partial x} \right] - A_l \frac{\partial p_l}{\partial x} + \rho_l A_l g \sin\theta - \frac{1}{2} P_{lw} \rho_l {u_l}^2 f_{lw} - \frac{1}{2} P_i \rho_l {u_l}^2 f_{il} = \rho_l A_l \frac{\partial u_l}{\partial t} \quad (9)$$

The Vapor Energy Equation

For the evaporator section:

$$A_v \frac{\partial E_v}{\partial t} + \frac{\partial}{\partial x}[u_v A_v (E_v + p_v)] = \frac{\partial}{\partial x}\left\{ \frac{4}{3} \mu_v u_v A_v \frac{\partial u_v}{\partial x} + k_v A_v \frac{\partial T_v}{\partial x} \right\} + q P_{vw} + h_{fg} v_{vi} \rho_v P_{vi} + \frac{1}{2} \rho_v {u_v}^2 f_{vi} u_v P_{vi} + \frac{1}{2} \rho_v {u_v}^2 f_{vw} u_v P_{vw} \quad (10)$$

For the adiabatic section:

$$A_v \frac{\partial E_v}{\partial t} + \frac{\partial}{\partial x}[u_v A_v (E_v + p_v)] = \frac{\partial}{\partial x}\left\{ \frac{4}{3} \mu_v u_v A_v \frac{\partial u_v}{\partial x} + k_v A_v \frac{\partial T_v}{\partial x} \right\} + \frac{1}{2} \rho_v {u_v}^2 f_{vi} u_v P_{vi} + \frac{1}{2} \rho_v {u_v}^2 f_{vw} u_v P_{vw} \quad (11)$$

For the condenser section:

$$A_v \frac{\partial E_v}{\partial t} + \frac{\partial}{\partial x}[u_v A_v (E_v + p_v)] = \frac{\partial}{\partial x}\left\{ \frac{4}{3} \mu_v u_v A_v \frac{\partial u_v}{\partial x} + k_v A_v \frac{\partial T_v}{\partial x} \right\} - h_0 P_{vw} \Delta T - h_{fg} v_{vi} \rho_v P_{vi} + \frac{1}{2} \rho_v {u_v}^2 f_{vi} u_v P_{vi} + \frac{1}{2} \rho_v {u_v}^2 f_{vw} u_v P_{vw} \quad (12)$$

The Liquid Energy Equation:

For the evaporator section:

$$A_l \frac{\partial E_l}{\partial t} + \frac{\partial}{\partial x}[u_l A_l (E_l + p_l)] = \frac{\partial}{\partial x}\left\{ \frac{4}{3} \mu_l u_l A_l \frac{\partial u_l}{\partial x} + k_l A_l \frac{\partial T_l}{\partial x} \right\} + q P_{lw} - h_{fg} v_{li} \rho_l P_{li} + \frac{1}{2} \rho_l {u_l}^2 f_{lvi} u_l P_{li} + \frac{1}{2} \rho_l {u_l}^2 f_{lw} u_l P_{lw} \quad (13)$$

For the adiabatic section:

$$A_l \frac{\partial E_l}{\partial t} + \frac{\partial}{\partial x}[u_l A_l (E_l + p_l)] = \frac{\partial}{\partial x}\left\{ \frac{4}{3} \mu_l u_l A_l \frac{\partial u_l}{\partial x} + k_l A_l \frac{\partial T_l}{\partial x} \right\} + \frac{1}{2} \rho_l {u_l}^2 f_{lvi} u_l P_{li} + \frac{1}{2} \rho_l {u_l}^2 f_{lw} u_l P_{lw} \quad (14)$$

For the condenser section:

$$A_l \frac{\partial E_l}{\partial t} + \frac{\partial}{\partial x}[u_l A_l (E_l + p_l)] = \frac{\partial}{\partial x}\left\{ \frac{4}{3} \mu_l u_l A_l \frac{\partial u_l}{\partial x} + k_l A_l \frac{\partial T_l}{\partial x} \right\} - h_0 P_{lw} \Delta T + h_{fg} v_{li} \rho_l P_{li} + \frac{1}{2} \rho_l {u_l}^2 f_{lvi} u_l P_{li} + \frac{1}{2} \rho_l {u_l}^2 f_{lw} u_l P_{lw} \quad (15)$$

The equation of state:

$$p_v = \rho_v R_v T_v \quad (16)$$

The Hagen-Poiseuille equation

$$\frac{\partial p_l}{\partial x} = -\frac{8 \mu_l u_l}{\left(\frac{{D_H}^2}{4} \right)} \quad (17)$$

The physical system under analysis is shown in Fig. 2. The boundary conditions prescribed at the beginning of the evaporator and at the end of the condenser are:

At x = 0 and L, for all t,

$$u_v = u_l = 0$$

$$\frac{\partial T}{\partial x} = 0$$

For x=0

$$r = r_{min}$$

where, r_{min} is the minimum meniscus radius which is obtained from the literature.

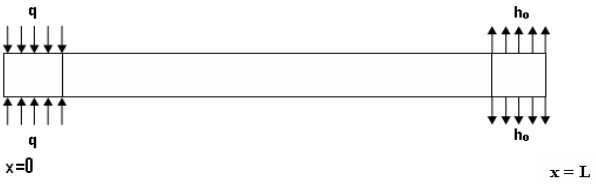

Fig. 2 The physical system under analysis

$$p_v - p_l = \frac{\sigma}{r_{min}} \quad (18)$$

At t = 0, for all x,

$$p_v = p_l = p_{sat}$$
and $$T_v = T_l = T_{sat}$$

The friction factors in the governing equations can be generally expressed as

$$f = \frac{\kappa}{R_e} \quad (19)$$

where *k* is a constant that depends on the geometry of the heat pipe channel. The important area parameters and their calculations are shown in Fig. 3.

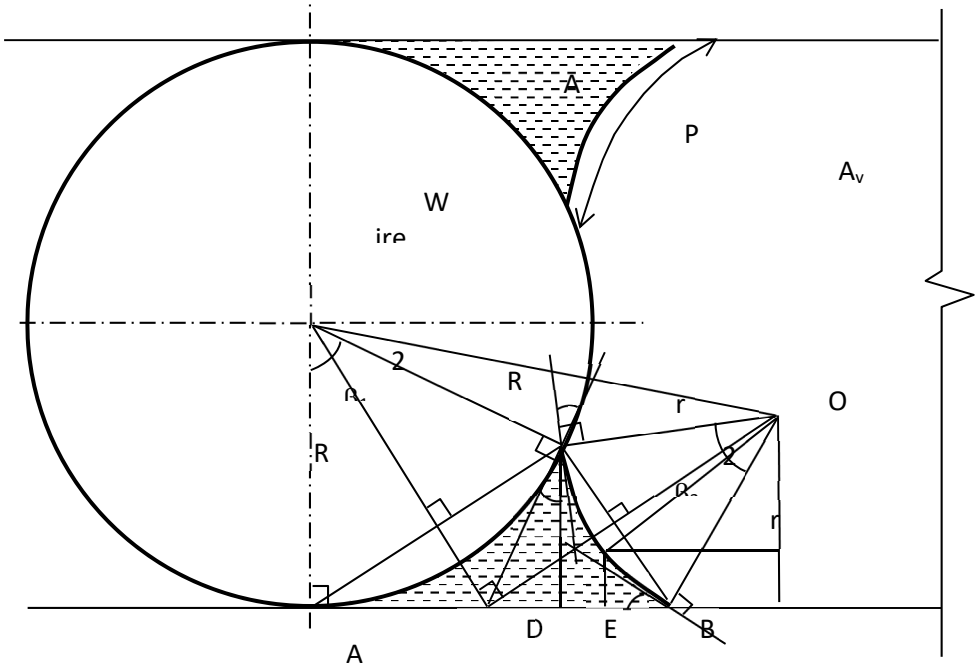

Fig. 3 Geometry of the interface meniscus in the wire-bonded micro heat pipe (Rag and Sobhan, 2009; Rag and Sobhan, 2010; Rag *et al.*, 2018).

The area of the liquid considering all four corners can be derived as

$$A_l = 8R_w r Sin\beta_1 Sin\beta_2 - 4{R_w}^2(\beta_1 - Sin\beta_1 Cos\beta_1) - 4r^2(\beta_2 - Sin\beta_2 Cos\beta_2) \quad (20)$$

The area of the vapor is

$$A_v = R_w(2P_w - \pi R_w) - A_l \quad (21)$$

where P_w is the pitch of the wires.

The liquid-vapor interface perimeters are P_{iv} and P_{il}

$$P_{iv} = P_{il} = 8r\beta_2 \quad (22)$$

The liquid wetted perimeter

$$P_l = 2R_w(\beta_1 + tan\,\beta_1) \quad (23)$$

The vapor wetted perimeter

$$P_v = 2(P_w + \pi R_w) + 8(r\beta_2 - R_w\,tan\,\beta_1 - R_w\beta_1) \quad (24)$$

The governing equations can be solved numerically. The procedure for solution can be summarized as follows:

1. The local meniscus radius is obtained using the Laplace – Young equation.
2. The vapor momentum equation is used to obtain the axial vapor velocity.
3. The interfacial vapor velocity is obtained using the vapor continuity equation and the interfacial liquid velocity is calculated applying the mass balance at the interface.
4. The vapor temperature is obtained from the vapor energy equation.
5. The vapor pressure is calculated using the equation of state for the vapor. It is again substituted in the vapor momentum equation and iterated for spatial convergence.
6. From the liquid continuity equation, the liquid velocity derivatives are obtained in terms of the interfacial liquid velocity. These were substituted in the liquid momentum

equation. The liquid momentum equation is solved to obtain the axial liquid velocity.

7. The liquid pressure is calculated using the Hagen- Poiseuille equation. The value of the liquid pressure is again substituted in the liquid momentum equation, and iterated for spatial convergence.
8. The liquid temperature is obtained from the liquid energy equation.
9. The time stepping is continued to obtain steady-state results.

Successive under relaxation is used in the computation for getting converged results of all the field variables. Computational accuracy was obtained by successive refinement of the space and time steps.

2.3 Experimental Validation

A wire-bonded micro heat pipe was fabricated corresponding to the dimensions of a base-line case utilized in the computation, and tested, in order to validate the computational results. An experimental test facility in which multiple functions of evacuation and charging of the wire-bonded micro heat pipe, as well as obtaining the surface temperature distribution through thermocouple measurement was fabricated, as shown in Fig. 4.

The dimensions of the micro heat pipe were similar to the values used in computations, such that the evaporator section was 20 mm x 20 mm, the adiabatic section was 85 mm x 20 mm and the condenser section was 20 mm x 20 mm. In order to supply heat to the evaporator section, an electrical heater coil made of Tungsten wire of 1.5 mm diameter wound over a layer of mica (electrical insulation) was used. Maintaining a vacuum of 60 Torr the heat pipe was charged with 1 ml

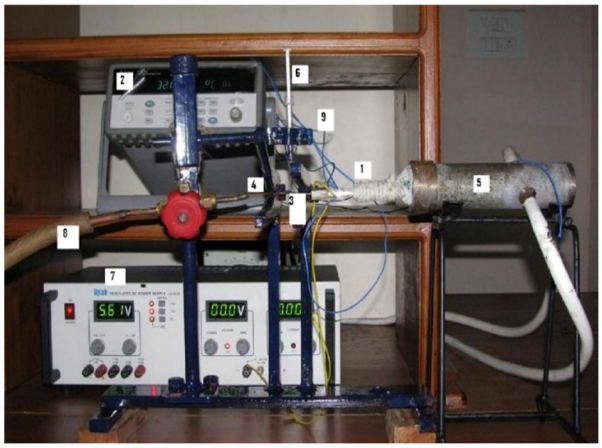

Fig. 4 Photograph of the experimental test facility

1. Wire-bonded micro heat pipe array 2. Data Logger 3. Flexible rubber tube 4. Copper capillary tube 5. Water bath 6. Charging line 7. Multi power unit 8. Evacuation line 9. Thermocouple wires

of deionized water, which provided 110% of the predetermined charge of working fluid. The voltage and current were adjusted using a multi-power unit to obtain heater outputs of 1 W/cm^2, 1.5 W/cm^2 and 2 W/cm^2 applied to the surface of the evaporator. The calibrated thermocouples were attached at various points longitudinally on the heat pipe surface –at the midpoint of the evaporator, at the junction between the evaporator and the adiabatic section, at the midpoint of the adiabatic section, at the junction between the adiabatic section and the condenser, and at the midpoint of the condenser.

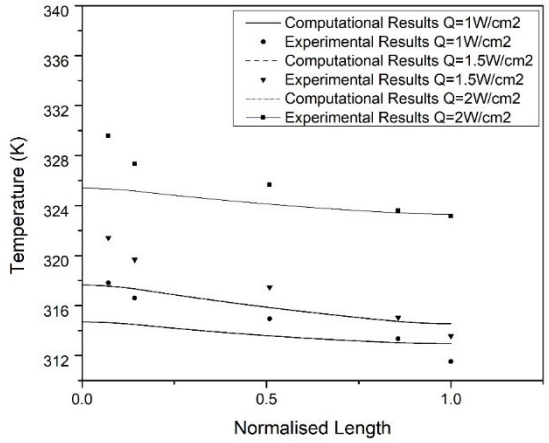

Fig. 5 Comparison of experimental and computational results (Rag *et al.*, 2018)

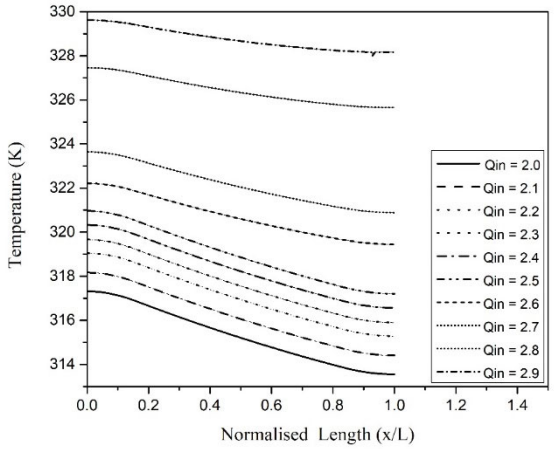

Fig. 6 Effect of input heat flux on the steady-state temperature distribution (Rag *et al.*, 2018)

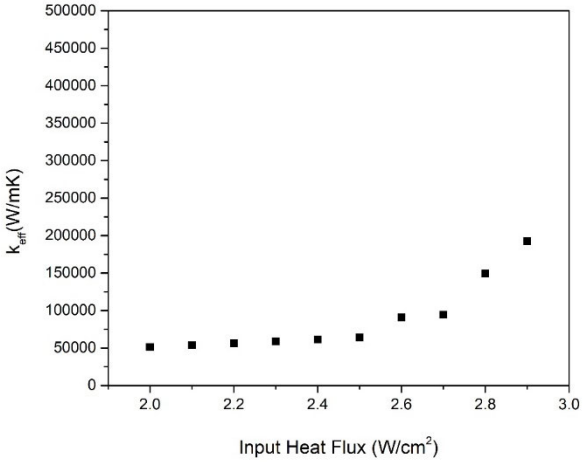

Fig. 7 Variation of effective thermal conductivity with input heat flux (Rag *et al.*, 2018)

The temperatures obtained in each case are plotted and compared with the computational results with the same input heat flux and a condenser heat transfer coefficient of 650 W/m^{2}K in Fig. 5. The experimental results obtained are illustrated and compared with the computational results. It should be noted that the experimental data pertain to the outer surface of the heat pipe, and the theoretical results are for the fluid inside. Though the temperature drop across the case can be estimated, using the known heat flux, the accuracy of such a calculation would be questionable, as there are many variables in picture.

The analysis of the wire bonded micro heat pipes yielded a number of computational results on its performance, which have been presented in the literature (Rag and Sobhan, 2009;2010; Rag *et al.*, 2018). Typical results of the computational study are illustrated in Fig. 6 and Fig. 7.

3. ADVANCES ON THE WIRE- BONDED DESIGN

Various designs of wire bonded heat pipes for heat dissipation from different systems have been developed and reported in the literature. There have been developments aimed at study of the processes involved, as well as application of the device in various physical systems. Though the physical shapes and functional arrangements have been different in some of the cases, the principle of operation of these systems have all been similar. Select designs are reviewed discussed below.

Launay *et al.* (2004) presented an experimental and theoretical investigation of a copper – water wire-plate micro heat pipe array. An improvement in the effective thermal conductivity by a factor of 1.3 was achieved, compared to an empty micro heat pipe array. A numerical model was also developed in order to predict the temperature field and the maximum heat flux corresponding to the capillary limit, based on the conservation equations for the liquid and vapor phases. The wall temperatures were calculated using the thermal network of the wall and the liquid film. The effects of the contact angle, fluid type, corner angle and fill charge were theoretically investigated. The analysis showed a good agreement between the theoretical and experimental data. Fig. 8 shows a comparison of the theoretical and experimental temperature variations along the heat pipe.

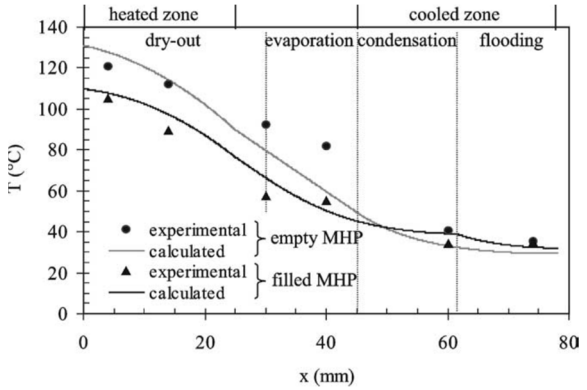

Fig. 8 Comparison of the experimental and calculated temperatures for the charged and empty MHPs (Q=10 W) (Launey *et al.*, 2004).

Le Berre et al. (2003) reported fabrication details and experimental investigations of silicon micro heat pipes for electronics cooling application. A study based on thermal and hydrodynamic models for flat micro heat pipes, aimed at cooling of electronic components, was presented by Lefevre and Lallemand (2006). This consisted of analytical solutions for liquid and vapor flows inside the micro heat pipe and the temperature inside the wall. The capillary structure inside the micro heat pipe was modeled as a porous medium. The thermal model was able to calculate the conduction heat flux in the heat pipe wall separately from the phase change heat transfer.

Hung and Seng (2011) performed an analysis of the effects of the geometric design and the thermal performance of micro pipes where the fluid passage was in the form of star-grooves, as shown in Fig. 9. A one-dimensional, steady-state mathematical model was developed, primarily to obtain the effects of geometrical variations on the heat transport capacity and the optimal charge level.

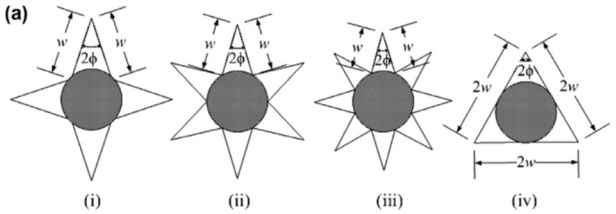

Fig. 9 Geometry of different cross-sectional shape of micro-heat pipes: (i) square star groove, (ii) hexagonal star groove, (iii) octagonal star groove and (iv) equilateral triangle (Hung and Seng, 2011).

The model was solved numerically to obtain the heat and fluid flow characteristics of the micro heat pipe. The effects of the geometrical parameters on the performance were obtained, and a comparison of the star-grooved and regular polygonal micro heat pipes was made. Under identical working condition, the star-grooved heat pipe was found to outperform the regular polygonal micro heat pipe due to its flexibility in reducing the corner apex angle for providing higher capillarity.

The thermal performance of a copper wire-bonded heat pipe was investigated experimentally by Chen *et al.* (2013). Water, ethanol and nanofluids were used as working fluids. The wire diameter was found to have an important effect on the heat transfer coefficient, but no significant impact on the maximum heat flux. The gap between the wires showed an important effect on both the heat transfer coefficient as well as the maximum heat flux. Use of nanofluid as the working fluid was found to improve the heat transfer performance of the wire bonded heat pipe. A concentration of 1.0 wt% was found to give the best heat transfer performance. The study investigated the effects of the liquid charging ratio, the wire diameter, the gap between the wires, and the mass concentration of the working fluids.

Paiva and Mantelli (2015a) proposed a technology which consists of covering the internal surfaces of the casing plates of the heat pipe in the evaporator region, with layers of sintered metal powder wicks, while the wick of the adiabatic and condenser sections consist of grooved structures. The wick structures of the adiabatic and condenser sections consisted of grooved structures sandwiched between the metallic plates of the casing, and wire welded by diffusion process. This technology associated the high liquid pumping capacity of sintered metal powder structures with low liquid pressure drop of diffusion welded wire-plate grooves. Several hybrid heat pipes were designed, and were found to compare well with the theoretical models. Among the parameters that affect the thermal performance, the most important were the geometry of the porous medium and the inventory of the working fluid. The thermal model developed in the work reproduced the temperature distribution along the heat pipe very well. In another paper, Paiva and Mantelli (2015b) used two models, namely a hydrodynamic model and a thermal model to perform a theoretical study of the wire-plate mini heat pipe. The temperature distribution along the heat pipe was predicted using a thermal model. A parametric study of the influence of the design parameters in the heat transfer performance was made. The maximum heat transfer capacity of the heat pipe was determined using the models. The influence of the wire diameter, wire spacing and working fluid in the thermal performance of such devices was studied. The results from the models were compared favorably with experimental data.

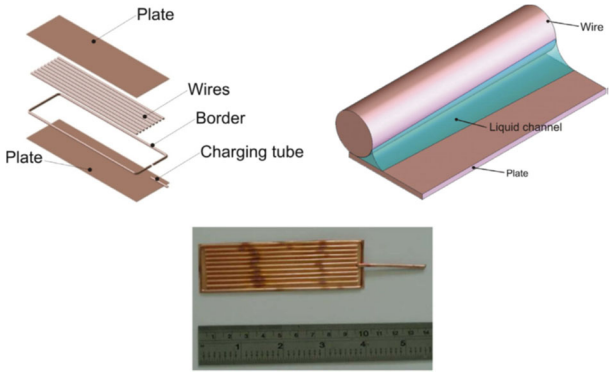

Fig. 10 Wire – plate mini heat pipe (Paiva and Mantelli, 2015a)

Wang *et al.* (2016) reported an experimental study on a wire bonded mesh screen flat heat pipe. Water and nanofluids were used as the working fluids. The influences of the working fluid, its mass concentration and the operating pressure on the thermal performance of the heat pipe were investigated. The thermal performance of the wire-bonded mesh screen heat pipe was found to be better than the wire-bonded flat heat pipe. It is also found that the use of the nanofluid significantly enhances the thermal performance of the heat pipe, and the enhancement of the heat transfer coefficient and the maximum heat flux increases with the mass concentration of the nanofluid up to 1.0%. Microphotograph of stainless-steel mesh surface after the nanofluid test showed that a loose coating of nanoparticles is formed on the mesh surface for some kinds of nanoparticles such as CuO, as shown in Fig. 11, and nanofluids with such nanoparticles were selected for the study. The coating layers formed by nanoparticles on the wall, metal wires and mesh screen enhance the micro groove structure and reduce the solid–liquid contact angle. All of these effects further increase the capillary force, and improve the convective heat transfer in micro groove structure.

.

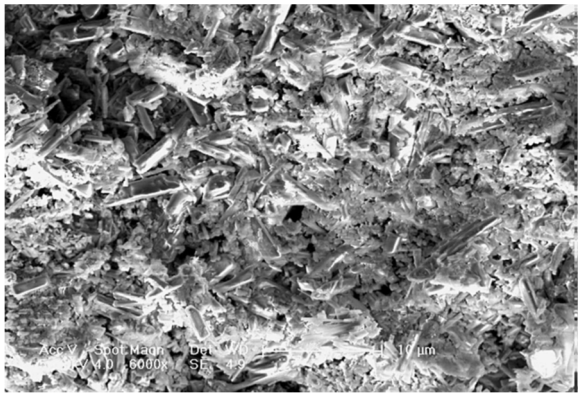

Fig. 11 Microphotograph of mesh after the nanofluid test (20 nm Cu, 1 wt%

Qu *et al.* (2017) reported investigations on the Heat transfer characteristics of micro-grooved oscillating heat pipes (OHPs). Microgroove (micro- fin) structure was introduced into the oscillating heat pipe (normally fabricated using wickless capillary tubes) to improve its heat transfer performance. The heat transfer characteristics of these micro grooved, oscillating heat pipes were experimentally investigated. The heat pipes were fabricated from copper tubes and used deionized water as the working fluid, with a filling ratio of 50%. Experiments showed that the microgroove structure provided significant improvement in the performance of the oscillating heat pipe. The effective thermal conductivity of a typical micro-grooved OHP was about 216 times higher than bulk copper material. The heat transfer enhancement of micro-grooved OHPs could be attributed to the phase-change intensification, the rotary motion of working fluid, and the enhanced liquid backflow to the evaporator due to the capillary action in the structure. The micro-grooved OHPs could be a promising option for applications of high energy utilization and high conversion efficiency.

Chen *et al.* (2016) presented a review of small heat pipes for applications related to cooling of electronics. Mini/micro heat pipes which are preferred for their high effectiveness and small dimensions, suitable for the compact structure and compatible processes with semi-conductor devices were described. The possibility of silicon as a preferred material for mini/micro heat pipes, and polymer based small heat pipes as attractive options for further development as they are inexpensive and easy to fabricate were considered. Possibility of nano-wicks such as carbon nanotubes due to their outstanding characteristics were also discussed. The review presented discussion on small heat pipes including their design, analysis and fabrication. An extensive review of the recent advances in MEMS based micro heat pipes has been presented by Qu *et al.* (2017). This novel technology was considered as a promising choice for thermal management applications in various microelectronics applications. The work includes a comprehensive review of the recent developments in MEMS type micro heat pipes, the fabrication and packaging methodologies used are summarized and the methods compared. The paper also presents some promising and innovative applications of MEMS based micro heat pipes, and discusses the challenges in the development and application of MEMS based micro heat pipes.

4. CONCLUSIONS

Micro heat pipes are promising devices for heat removal from various miniature devices such as electronic components, due to their small sizes, high effective thermal conductance, and passive operation. The wire-bonded micro heat pipe array is a relatively novel and non-conventional type of micro heat pipe which can find effective use especially in the thermal management of microelectronic devices. This device was fabricated by sandwiching an array of wires between two thin metal plates, making the passages formed between the wires act as the micro heat pipe channels. The sharp corners formed at the junction of the wires and the metal plates serve as the arteries for liquid transport from the condenser section to the evaporator section of the device. The most attractive aspect of this design is its ease of fabrication by sandwiching an array of wires between two metal plates.

These wire-bonded micro heat pipes have been tested and found to be very useful due to the ease of manufacture and the application potential, however, they have not as yet been widely adopted. The main objective of this paper has been to describe the construction and operation of the device, based on the literature already available. The development and the operating principle of the passive heat transport device has been explained, with important results cited from the literature. Various forms of the wire-bonded micro heat pipe design that have been utilized are described from a review of the published work in the literature. The device has been found to be effective, and could be utilized extensively for heat dissipation from compact devices efficiently. The objective of this work was mainly to describe the applicability of this device as a means of heat dissipation and to cite investigations where it has been used effectively as a promising heat transport device.

Nomenclature

A area of cross-section, m^2
C specific heat, J/kg K

D characteristic dimension, m
D_H hydraulic diameter of the channel, m
E total energy per unit volume, J/m^3
f friction factor
g acceleration due to gravity, m/s^2
h_{fg} latent heat of vaporization, J/kg
h_0 heat transfer coefficient, W/m^{2}K
k thermal conductivity, W/mK
Kn Knudsen number
l length of a section, m
L length of the heat pipe, m
p pressure, Pa
P perimeter, m
P_w pitch of the wires (center to center distance of the wires), m
q heat flow rate, W/m^2
Q heat, W
r radius of the meniscus, m
r_h hydraulic radius of the channel, m
r_{min} minimum meniscus radius, m
R Universal gas constant, J/kg K
Re Reynolds number
R_w radius of the wire, m
t time, s
T temperature, K
ΔT terminal temperature drop, T-$T_{amb,}$ K
u axial velocity, m/s
v velocity, m/s
x axial coordinate

Greek Symbols
α contact angle, deg.
β_1 half-angle of contact arc of liquid with wire, grade
β_2 half-angle of liquid curvature, grade
κ geometrical constant
λ mean free path of the vapor, m
μ dynamic viscosity, kg/m s
ρ density, kg/m^3
σ surface tension, N/m
θ inclination angle, deg
τ Shear stress, N/m^2

Subscripts
a adiabatic section
amb ambient
c condenser section
cs cross-section
e evaporator section
eff effective
h hydraulic
i interface
l liquid
li liquid-interface
lw liquid-wall
sat saturation
v vapor
vi vapor interface
vw vapor-wall

REFERENCES

Babin, B. R., Peterson, G. P., and Wu. D., 1990, "Steady-state Modeling and Testing of a Micro Heat Pipe," *J. Heat Transfer*, **112**, 595-601.
https://doi.org/10.1115/1.2910428

Badran, B., Gerner, F.M., Ramadas, P., Henderson, H.T., and Baker, K.W., 1993, "Liquid Metal Micro Heat Pipes," Proc. *29th National Heat Transfer Conference*, Atlanta, Georgia HTD 236, 71-85.

Cao, Y and Faghri, A., 2017, "A Review on Micro/Miniature Heat Pipes," *J Enhanced Heat Transfer*, **24**, Issue 1-6, 473-482.
https://doi.org/10.1615/JEnhHeatTransf.v24.i1-6.340

Cao, Y. and Faghri, A., 1994, "Micro/Miniature Heat Pipes and Operating Limitations," *Journal of Enhanced Heat Transfer*, **1**, 265-274.
https://doi.org/10.1615/JEnhHeatTransf.v1.i3.80

Cao, Y., Faghri, A., and Mahefkey, E.T., 1993, "Micro/miniature Heat Pipes and Operating Limitations," *ASME-Publications-HTD* 236, 55.

Chen, X., Ye, H., Fan, X., Ren, T., and Zhang, G., 2016, "A Review of Small Heat Pipes for Electronics," *Applied Thermal Engineering*, **96**, 1-17.
https://doi.org/10.1016/j.applthermaleng.2015.11.048

Chen, Y. J, Wang, P. Y, Liu, Z. H, and Li, Y.Y., 2013, "Heat Transfer Characteristics of a new type of Copper Wire-bonded Flat Heat Pipe using Nanofluids," *International Journal of Heat and Mass Transfer*, **67**, 548-559.
https://doi.org/10.1016/j.ijheatmasstransfer.2013.08.060

Cotter, T. P. 1984. "Principles and Prospects of Micro Heat Pipes," *Proc. 5th Intl. Heat Pipe Conf.* Tsukuba, Japan, 328-335.

Do, K. H., Kim, S. J., and Garimella, S. V, 2008, "A Mathematical Model for Analyzing the Thermal Characteristics of a Flat Micro Heat Pipe with a Grooved Wick," *International Journal of Heat and Mass Transfer,* **51**, 4637-4650.
http://dx.doi.org/10.1016/j.ijheatmasstransfer.2008.02.039-

Duncan, A.B. and Peterson, G. P., 1995, "Charge Optimization for a Triangular Shaped Etched Micro Heat Pipe," *AIAA J. Thermophysics and Heat Transfer*, **9**, 365-368.
https://doi.org/10.2514/3.670

Faghri, A., 2014, "Heat Pipes: Review, Opportunities and Challenges," Frontiers in Heat Pipes, 5, 1-48.
https://doi.org/10.5098/fhp.5.1

Faghri, A., 2002, "Advances and Challenges in Micro/Miniature Heat Pipes," *Annual Review of Heat Transfer*, **12**, 1-25.
https://doi.org/10.1615/AnnualRevHeatTransfer.v12.30

Gerner, F. M., Longtin, J. P., Ramadas, P., Henderson, T.H., and Chang, W. S., 1992, "Flow and Heat Transfer Limitations in Micro Heat Pipes," *Proc. 28th National Heat Transfer Conference*, San Diego, CA. August 9-12.

Hung, Y. M., and Seng, Q., 2011, "Effects of Geometric Design on Thermal Performance of Star-Groove Micro-Heat Pipes," *Int'l Journal of Heat and Mass Transfer*, **54**, 1198-1209.
https://doi.org/10.1016/j.ijheatmasstransfer.2010.09.070

Khrustalev D., and Faghri, A., 1994, Thermal Analysis of a Micro Heat Pipe, *J Heat Transfer*, ASME, **116**, 189-198. https://doi.org/10.1115/1.2910855

Launay, S., Sartre, V., Mantelli, M. B. H., de Paiva, K. V., and Lallemand, M., 2004, "Investigation of a Wire Plate Micro Heat Pipe Array," *Int'l Journal of Thermal Sciences*, 43, 499-507. https://doi.org/10.1016/j.ijthermalsci.2003.10.006

Le Berre, M, Lunay, S, Sartre, V and Lallemand, M., 2003, "Fabrication and Experimental Investigation of Silicon Micro Heat Pipes for Cooling Electronics," *J Micromechanics and Microengineering,* **13**, 436-441. http://dx.doi.org/10.1088/0960-1317/13/3/313

Lefe'vre, F., and Lallemand, M., 2006, "Coupled Thermal and Hydrodynamic Models of Flat Micro Heat Pipes," *International Journal of Heat and Mass Transfer*, **49**, 1375-1383. https://doi.org/10.1016/j.ijheatmasstransfer.2005.10.001

Longtin, J. P., Badran, B., and Gerner F.M., 1994, "A One-dimensional Model of a Micro Heat Pipe during Steady-state Operation," *J. Heat Transfer*, **116**, 709-715. https://doi.org/10.1115/1.2910926

Paiva, K. V., and Mantelli, M. B. H., 2015a, "Theoretical Thermal Study of Wire-Plate Mini Heat Pipes," *International Journal of Heat and Mass Transfer*, **83**, 146-163. https://doi.org/10.1016/j.ijheatmasstransfer.2014.11.049

Paiva, K. V., and Mantelli, M. B. H., 2015b, "Wire-plate and Sintered Hybrid Heat Pipes: Model and Experiments," *International Journal of Thermal Sciences,* **93**, 36-51. https://doi.org/10.1016/j.ijthermalsci.2015.01.037

Peterson, G. P. and Ma, H. B., 1999, "Temperature Response of Heat Transport in Micro Heat Pipes," *J. Heat Transfer*, **121**, 438- 445. https://doi.org/10.1115/1.2825997

Peterson, G. P. and Ma, H.B., 1996, "Theoretical Analysis of the Maximum Heat Transport in Triangular Grooves: A Study of Idealized Micro Heat Pipes," *J. Heat Transfer*, **118**, 731 - 39. https://doi.org/10.1115/1.2822693

Peterson, G.P., 1988, "Investigation of Miniature Heat Pipes", Final Report, Wright Patterson AFB, Contract No. F33615 86 C 2733, Task 9.

Peterson, G.P., and Wang, Y. X., 2003, "Flat Heat Pipe Cooling Devices for Mobile Computers," *IMECE*, Washington DC.

Qu, J.,Wu, H., Cheng, P., Wang, Q., and Sun, Q., 2017, "Recent Advances in MEMS-Based Micro Heat Pipes," *International Journal of Heat and Mass Transfer*, **110**, 294-313. https://doi.org/10.1016/j.ijheatmasstransfer.2017.03.034

Qu. J., Li. X., Wang, Q., Liu, F., and Guo, H., 2017, "Heat Transfer Characteristics of Micro-Grooved Oscillating Heat Pipes," *Experimental Thermal and Fluid Sciences*, **85**, 75-84. https://doi.org/10.1016/j.expthermflusci.2017.02.022

Rag, R. L., and Sobhan, C. B., 2010, "Computational Analysis and Optimization of Wire - Sandwiched Micro Heat Pipes," *International Journal of Micro-Nano Scale Transport*, Multi-Science Publishing, **1**, 57-78. https://doi.org/10.1260/1759-3093.1.1.57

Rag, R. L., and Sobhan, C. B., 2009, "Computational Analysis of Fluid Flow and Heat Transfer in Wire-bonded Micro Heat Pipes," *AIAA J. Thermophysics and Heat Transfer*, **23**, 741-751. https://doi.org/10.2514/1.44101

Rag, R. L., Sobhan, C. B. and Peterson, G. P., 2018, "Computational Analysis of Wire-Bonded Micro Heat Pipe: Influence of Thermophysical Parameters," *AIAA J. Thermophysics and Heat Transfer*, **32**, 925-932. https://doi.org/10.2514/1.T5359

Wang, P. Y., Chen, Y. J., and Liu, Z. H., 2016, "Performance Improvement of Wire-Bonded Mesh Screen Flat Heat Pipe using Water-Based Nanofluid," *Heat Mass Transfer*, **52**, 2609-2619. https://doi.org/10.1007/s00231-016-1758-9

Wang, Y. X., and Peterson, G. P., 2002a, "Analysis of Wire - Bonded Micro Heat Pipe Arrays," AIAA. *Journal of Thermophysics and Heat Transfer*, **16**, 346-355. https://doi.org/10.2514/2.6711

Wang, Y. X., and Peterson, G. P., 2002b, "Optimization of Micro Heat Pipe Radiators in a Radiation Environment," *AIAA J. Thermophysics and Heat Transfer*, **16**, 537-546. https://doi.org/10.2514/2.6729

Wang, Y., Ma, H. B., and Peterson, G. P., 2001, "Investigation of the Temperature Distributions on Radiator Fins with Micro Heat Pipes," *AIAA J. Thermophysics and Heat Transfer*, **15**, 42-49. https://doi.org/10.2514/2.6577

Wu, D. and Peterson, G. P. 1991, "Investigation of the Transient Characteristics of a Micro Heat Pipe," *AIAA J. Thermophysics and Heat Transfer*, **5**, 129-134. https://doi.org/10.2514/3.239